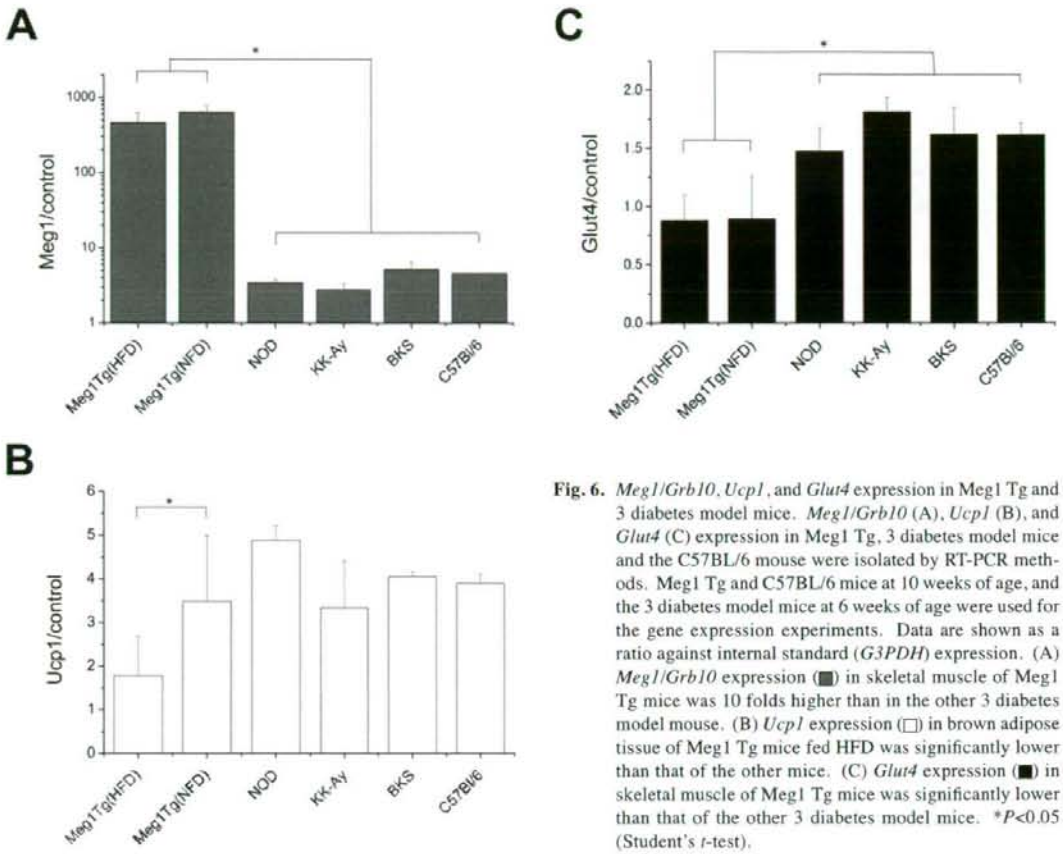

Fig. 6. *Meg1/Grb10*, *Ucp1*, and *Glut4* expression in Meg1 Tg and 3 diabetes model mice. *Meg1/Grb10* (A), *Ucp1* (B), and *Glut4* (C) expression in Meg1 Tg, 3 diabetes model mice and the C57BL/6 mouse were isolated by RT-PCR methods. Meg1 Tg and C57BL/6 mice at 10 weeks of age, and the 3 diabetes model mice at 6 weeks of age were used for the gene expression experiments. Data are shown as a ratio against internal standard (*G3PDH*) expression. (A) *Meg1/Grb10* expression (■) in skeletal muscle of Meg1 Tg mice was 10 folds higher than in the other 3 diabetes model mouse. (B) *Ucp1* expression (□) in brown adipose tissue of Meg1 Tg mice fed HFD was significantly lower than that of the other mice. (C) *Glut4* expression (■) in skeletal muscle of Meg1 Tg mice was significantly lower than that of the other 3 diabetes model mice. $^*P<0.05$ (Student's *t*-test).

ance (Fig. 3). The plasma insulin concentration of Meg1 Tg mice was significantly higher than in control mouse (Table 2). These data demonstrate that the dysregulation of plasma glucose was caused by insulin resistance. Our results provide support for Meg1 Tg mouse as a 2DM mouse model. Moreover, the body weights of Meg1 Tg neonates were slightly lower than controls, and this difference increased with growth up to 12 to 15% of body weight. BMI of Meg1 Tg mice was also smaller than control mice (Figs. 1 and 2). Body, visceral fat weight and liver weights were also slightly lower in Meg1 Tg mice than in control mice. However, the visceral fat/body weight and liver/body weight ratios of Meg1 Tg mice were similar to those of control mice (Table 1). Overall, the Meg1 Tg mouse showed a non-obese mouse character.

There are several spontaneous polygenic models of 2DM, such as the OLETF rat, the KK-A^y mouse, the NSY mouse, and the BKS mouse, which develop overt obesity and hyperinsulinemia prior to the onset of diabetes [7, 14, 34]. The KK-A^y mouse and the BKS mouse showed obesity compared with controls [33, 35]. However, the Meg1 Tg mouse model showed a non-obese character. Only limited data exist for 2DM in Japanese subjects, probably because Japanese people are relatively lean. Some Japanese 2DM patients are non-obese patients and the causal factors of 2DM onset is being analyze by many laboratories [15, 28]. The Meg1 Tg diabetes mouse model may provide a useful tool for these researches.

Biochemical analysis data of the Meg1 Tg mouse demonstrated metabolic abnormality. Plasma BUN in

Meg1 Tg mice was significantly lower than in control mice. Plasma TG, insulin, adiponectin, and resistin levels of HFD-fed Meg1 Tg mice were significantly higher than those of control mice. The mean concentration of TG in Meg1 Tg mice, especially with HFD feeding, was over 200 mg/dl, a condition that is called high-fat plasma. High-fat plasma is said to be a precursor of diabetes [19]. A high level of plasma adiponectin and low BMI were found in Meg1 Tg mice fed HFD (Fig. 2B). There was an inverse correlation between plasma adiponectin and BMI in the Meg1 Tg mouse (data not shown). This shows that the Meg1 Tg mouse has characteristics similar to human 2DM. The circulating IGF-1 level in Meg1 Tg mice tended to be lower than that of control mice (Table 2). A lower IGF-1 level could explain the lower body weight of the Meg1 Tg mouse due to the role of IGF-1 signaling in postnatal growth [10]. Overall, the biochemical data suggest that HFD feeding in the Meg1 Tg mouse induces human 2DM related characteristics. In a comparison of the biochemical data between the Meg1 Tg mouse and other 2DM model mice, such as KK-A^y and BKS mouse, the Meg1 Tg mouse did not show plasma insulin and a remarkable rise of plasma glucose levels like KK-A^y and BKS mice, but showed a property that is characteristic of human 2DM, a rise of adiponectin level [5, 16, 18]. In addition, it is a very unique characteristic that this property is caused by environmental factors such as diet.

In mRNA expression analysis, diabetes related genes, such as *Grb10*, *Ucp1*, and *Glut4*, in the Meg1 Tg mouse were compared with 3 famous diabetes mouse models (Fig. 6). Regarding the relationship between the *Meg1/Grb10* gene and the non-obese character of the Meg1 Tg mouse, overexpression of the *Meg1/Grb10* gene may hold the IGF-1 acceptor signal transduction system in check during development in the embryonic stage and the holding effect would be maintained until long after birth [31]. It is reported that maternal duplication of proximal chromosome 11 retards embryonic growth, whereas paternal duplication promotes growth [2]. A recent *Grb10* knockout study has clearly demonstrated that *Meg1/Grb10* is the gene responsible for embryonic overgrowth observed in paternal duplication of the chromosome 11 region [3], although the effect of *Meg1/Grb10* overproduction remains to be addressed. Our data may provide answers to these puzzling issues. Grb10 regulates the insulin signaling and sensitivity *in vivo* [36]. This suggests that a high level of the *Grb10* gene could affect insulin resistance in the Meg1 Tg mouse. The reduction in intracellular lipid by constitutive expression of *Ucp1* reflects down-regulation of fat synthesis rather than up-regulation of fatty acid oxidation [32]. The down-regulation of *Ucp1* in Meg1Tg mice fed HFD could explain the non-obese character of the Meg1 Tg mouse. The quantity of expression of *Glut4* mRNA in skeletal muscle decreased significantly in Meg1 Tg mice (Fig. 6C). GLUT4 translocation can be activated by insulin, to which the Meg1 Tg mouse has resistance, and may be related to the GLUT4 decrease in skeletal muscle.

Recently, association of hGrb10 genetic variations with 2DM in Caucasian subjects has been reported [2]. There is no evidence of such a correlation in Japanese subjects. However, it has been revealed that the expression of hGrb10 was influenced by epigenetic alterations. It is important to investigate hGrb10 expression and the relationship to environmental conditions including diet in 2DM model mice.

Acknowledgment(s)

We thank Ms. Tomoko Hata and Naho Takekawa for technical assistance.

References

1. Caroline, S.F., Michael, J.P., James, B.M., Ramachandran, S.V., Yamini, S.L., and Ralph, B.D. 2006. Trends in the incidence of type 2 diabetes mellitus from the 1970s to the 1990s. *Circulation* 113: 2914–2918.
2. Cattanach, B.M., Beechey, C.V., Rasberry, C., Jones J., and Papworth, D. 1996. Time of initiation and site of action of the mouse chromosome 11 imprinting effects. *Genet. Res.* 68: 35–44.
3. Charalambous, M., Smith, F.M., Bennett, W.R., Crew, T.E., Mackenzie, F., and Ward, A. 2003. Disruption of the imprinted *Grb10* gene leads to disproportionate overgrowth by an Igf2-independent mechanism. *Proc. Natl. Acad. Sci. U.S.A.* 100: 8292–8297.
4. Chu, K.Y., Lau, T., Carlsson, P.O., and Leung, P.S. 2006. Angiotensin II type 1 receptor blockade improves beta-cell function and glucose tolerance in a mouse model of type 2 diabetes. *Diabetes* 55: 367–374.
5. Combs, T.P., Wagner, J.A., Berger, J., Doebber, T., Wang,

W.-J., Zhang, B.B., Tanen, M., Berg, A.H., O'Rahilly, S., Savage, D.B., Chatterjee, K., Weiss, S., Larson, P.J., Gottesdiener, K.M., Gertz, B.J., Charron, M.J., Scherer, P.E., and Moller, D.E. 2002. Induction of adipocyte complement-related protein of 30 kilodaltons by PPARg agonists: a potential mechanism of insulin sensitization. *Endocrinology* 143: 998–1007.

6. Cramer, K.L., Gerrald, Q.D., Nichols, C.B., Price, M.S., and Alspaugh, J.A. 2006. Transcription factor Nrg1 mediates capsule formation, stress response, and pathogenesis in Cryptococcus neoformans. *Eukaryotic Cell* 5: 1147–1156.
7. DeChhiara, T.M., Robertson, E.J., and Efstratiadis, A. 1991. Parental imprinting of the mouse insulin-like growth factor II gene. *Cell* 64: 849–859.
8. Dey, B.R., Frick, K., Lopaczynski, W., Nissley, S.P., and Furlanetto, R.W. 1996. Evidence for the direct interaction of the insulin-like growth factor I receptor with IRS-1, Shc, and Grb10. *Mol. Endocrinol.* 10: 631–641.
9. Dong, L.Q., Du, H., Porter, S.G., Kolakowski, L.F., Lee, A.V., Mandarino, L.J., Fan, J., Yee, D., Liu, F., and Mandarino, J. 1997. Cloning, chromosome localization, expression, and characterization of an *Src* homology 2 and pleckstrin homology domain-containing insulin receptor binding protein hGrb10gamma. *J. Biol. Chem.* 272: 29104–29112.
10. Floria, L., Joseph, D.T., Kaechoong, L., Gino, V.S., Argiris, E. 2001. Roles of growth hormone and insulin-like growth factor 1 in mouse postnatal growth. *Dev. Biol.* 229: 141–162.
11. Furuya, Y., Tagami, S., Hasegawa, A., Ishii, J., Hirokawa, J., Yoshimura, H., Honda, T., Sakaue, S., Aoki, K., Murakami, M., Kudo, I., and Kawakami, Y. 1999. Increased glomerular cytosolic phospholipase A2 activity of OLETF rats with early diabetes. *Exp. Clin. Endocrinol. Diabetes* 107: 299–305.
12. Hanley, A.J., Karter, A.J., Williams, K., Festa, A., D'Agostino, R.B. Jr., Wagenknecht, L.E., and Haffner, S.M. 2005. Prediction of type 2 diabetes mellitus with alternative definitions of the metabolic syndrome: the Insulin Resistance Atherosclerosis Study. *Circulation* 112: 3675–3676.
13. Hattersley, A.T. 2004. Unlocking the secrets of the pancreatic beta cell: man and mouse provide the key. *J. Clin. Invest.* 114: 314–316.
14. Horio, F., Teradaira, S., Imamura, T., Anunciado, R.V., Kobayashi, M., Namikawa, T., and Niki, I. 2005. The HND mouse, a nonobese model of type 2 diabetes mellitus with impaired insulin secretion. *Eur. J. Endocrinol.* 153: 971–979.
15. Kanauchi, M. 2003. Comparison in renal histology between Japanese obese and non-obese microalbuminuric type 2 diabetic patients. *Nephrol. Dial. Transplant.* 18: 849–850.
16. Kawasaki, F., Matsuda, M., Kanda, Y., Inoue, H., and Kaku, K. 2005. Structural and functional analysis of pancreatic islets preserved by pioglitazone in *db/db* mice. *Am. J. Physiol. Endocrinol. Metab.* 288: E510–E518.
17. Kushi, A., Sasai, H., Koizumi, H., Takeda, N., Yokoyama, M., and Nakamura, M. 2006. Obesity and mild hyperinsulinemia found in neuropeptide Y-Y1 receptor-deficient mouse. *Proc. Natl. Acad. Sci. U.S.A.* 95: 15659–15664.
18. Kuwabara, K., Murakami, K., Todo, M., Aoki, T., Asaki, T., Murai, M., and Yano, J. 2004. A novel selective peroxisome proliferator-activated receptor a agonist, 2-methyl-c-5-[4-[5-methyl-2-(4-methyphenyl)-4-oxazolyl]butyl]-1,3-dioxane-r-2-carboxylic acid(NS-220), potently decreases plasma triglyceride and glucose levels and modifies lipoprotein profiles in KK-A^y mice. *J. Pharmacol. Exp. Ther.* 309: 970–977.
19. Lewis, G.F., O'Meara, N.M., Soltys, P.A., Blackman, J.D., Iverius, P.H., Pugh, W.L., Getz, G.S., and Polonsky, K.S. 1991. Fasting hypertriglyceridemia in noninsulin-dependent diabetes mellitus is an important predictor of postprandial lipid and lipoprotein abnormalities. *J. Clin. Endocrinol. Metab.* 72: 934–944.
20. Louvi, A., Accili, D., and Efstratiadis, A. 1997. Growth-promoting interaction of IGF-II with the insulin receptor during mouse embryonic development. *Dev. Biol.* 189: 33–48.
21. Ma, D., Shield, J.P., Dean, W., Leclerc, I., Knauf, C., Burcelin, R.R., Rutter, G.A., and Kelsey, G. 2004. Impaired glucose homeostasis in transgenic mouse expressing the human transient neonatal diabetes mellitus locus, TNDM. *J. Clin. Invest.* 114: 339–348.
22. Miao, G., Ito, T., Uchikoshi, F., Tanemura, M., Kawamoto, K., Shimada, K., Nozawa, M., and Matsuda, H. 2005. Development of islet-like cell clusters after pancreas transplantation in the spontaneously diabetic Torri rat. *Am. J. Transplant.* 5: 2360–2367.
23. Miyoshi, N., Kuroiwa, Y., Kohda, T., Shitara, H., Yonekawa, H., Kawabe, T., Hasegawa, H., Barton, S.C., Surani, M.A., Kaneko-Ishino, T., and Ishino, F. 1998. Identification of the *Meg1/Grb10* imprinted gene on mouse proximal chromosome 11, a candidate for the Silver–Russell syndrome gene. *Proc. Natl. Acad. Sci. U.S.A.* 95: 1102–1107.
24. Momose, K., Nunomiya, S., Nakata, M., Yada, T., Kikuchi, M., and Yashiro, T. 2006. Immunohistochemical and electron-microscopic observation of beta-cells in pancreatic islets of spontaneously diabetic Goto-Kakizaki rats. *Med. Mol. Morphol.* 39: 146–153.
25. Morrione, A., Valentinis, B., Resnicoff, M., Xu, S., and Baserga, R. 1997. The role of m*Grb10*alpha in insulin-like growth factor I-mediated growth. *J. Biol. Chem.* 272: 26382–26387.
26. Nakae, J., Kido, Y., and Accili, D. 2001. Distinct and overlapping functions of insulin and IGF-I receptors. *Endcr. Rev.* 22: 818–835.
27. O'Neill, T. J., Rose, D.W., Pillay, T.S., Hotta, K., Olefsky, J.M., and Gustafson, T.A. 1996. Interaction of a GRB-IR splice variant (a human GRB10 homolog) with the insulin and insulin-like growth factor I receptors. Evidence for a role in mitogenic signaling. *J. Biol. Chem.* 271: 22506–22513.
28. Ohki, Y., Kishi, M., Orimo, H., and Ohkawa, T. 2004. Insulin resistance in Japanese adolescents with type 2 diabetes mellitus. *J. Nippon Med. Sch.* 71: 88–91.
29. Paola, R.D., Ciociola, E., Boonyasrisawat, W., Nolan, D.,

Duffy, J., Miscio, G., Cisternino, C., Fini, G., Tassi, V., Doria, A., and Trischitta, V. 2006. Association of hGrb 10 genetic variations with type 2 diabetes in Caucasian subjects. *Diabetes Care* 29: 1181–1182.

30. Reynisdottir, I., Thorleifsson, G., Benediktsson, R., Sigurdsson, G., Emilsson, V., Einarsdottir, A.S., Hjorleifsdottir, E.E., Orlygsdottir, G.T., Bjornsdottir, G.T., Saemundsdottir, J., Halldorsson, S., Hrafnkelsdottir, S., Sigurjonsdottir, S.B., Steinsdottir, S., Martin, M., Kochan, J.P., Rhees, B.K., Grant, S.F., Frigge, M.L., Kong, A., Gudnason, V., Stefansson, K., and Gulcher, J.R. 2003. Localization of a susceptibility gene for type 2 diabetes to chromosome 5q34-q35.2. *Am. J. Hum. Genet.* 73: 323–335.
31. Shiura, H., Miyoshi, N., Konishi, A., Wakisaka-Saito, N., Suzuki, R., Muguruma, K., Kohda, T., Wakana, S., Yokoyama, M., Ishino, F., and Kaneko-Ishino, T. 2005. *Meg1/Grb10* overexpression causes postnatal growth retardation and insulin resistance via negative modulation of the IGF1R and IR cascades. *Biochem. Biophys. Res. Commun.* 329: 909–916.
32. Si, Y., Palani, S., Jayaraman, A., and Lee, K. 2007. Effects of forced uncoupling protein 1 expression in 3T3-L1 cells on mitochondrial function and lipid metabolism. *J. Lipid Res.* 48: 826–836.
33. Takada, Y., Takata, Y., Iwanishi, M., Imamura, T., Sawa, T., Morioka, H., Ishihara, H., Ishiki, M., Usui, I., Temaru, R., Urakaze, M., Satoh, Y., Inami, T., Tsuda, S., and Kobayashi, M. 1996. Effect of glimepiride (HOE 490) on insulin receptors of skeletal muscles from genetically diabetic KK-A^y mouse. *Eur. J. Pharmacol.* 308: 205–210.
34. Takeuchi, M., Itakura, A., Okada, M., Mizutan, S., and Kikkawa, F. 2006. Impaired insulin-regulated membrane aminopeptidase translocation to the plasma membrane in adipocytes of Otsuka Long Evans Tokushima Fatty rats. *Nagoya J. Med. Sci.* 68: 155–163.
35. Teixeira, S.R., Tappenden, K.A., and Erdman, J.W. Jr. 2003. Altering dietary protein type and quantity reduces urinary albumin excretion without affecting plasma glucose concentrations in BKS.Cg-+$Lepr^{db}$/+$Lepr^{db}$ (*db/db*) mouse. *J. Nutr.* 133: 673–678.
36. Wang, L., Balas, B., Christ-Roberts, C.Y., Kim, R.Y., Ramos, F.J., Kikani, C.K., Li, C., Deng, C., Reyna, S., Musi, N., Dong, L.Q., DeFronzo, R.A., Liu, F. 2007. Peripheral disruption of the *Grb10* gene enhances insulin signaling and sensitivity *in vivo*. *Mol. Cell. Biol.* 27: 6497–6505.
37. Wright, N.M., Metzger, D.L., Borowitz, S.M., and Clarke, W.L. 1993. Permanet neonatal diabetes mellitus and pancreatic agenesis. *Am. J. Dis. Child.* 147: 607–609.
38. Yi, L.Z., He, J., Liang, Y.Z., Yuan, D.L., and Chau, F.T. 2006. Plasma fatty acid metabolic profiling and biomarkers of type 2 diabetes mellitus based on GC/MS and PLS-LDA. *FEBS Lett.* 580: 6837–6845.
39. 1999–2001 National Health Interview Survey and 1999–2000 National Health and Nutrition Examination Survey estimates projected to year 2002. National Diabetes Fact Sheet, National Estimates on Diabetes. CDC publications and products.

Available online at www.sciencedirect.com
ScienceDirect
Virus Research 131 (2008) 170–179
Virus Research
www.elsevier.com/locate/virusres

The latent membrane protein 1 (LMP1) encoded by Epstein-Barr virus induces expression of the putative oncogene *Bcl*-3 through activation of the nuclear factor-κB

Hiroyuki Nakamura [a], Chihiro Ishii [a], Masakazu Suehiro [a], Akifumi Iguchi [b], Kazumichi Kuroda [b], Kazufumi Shimizu [b], Norio Shimizu [c], Ken-Ichi Imadome [a], Misako Yajima [a], Shigeyoshi Fujiwara [a,*]

[a] *Department of Infectious Diseases, National Research Institute for Child Health and Development, 2-10-1 Okura, Setagaya-ku, Tokyo 157-8535, Japan*
[b] *Department of Immunology and Microbiology, Nihon University School of Medicine, 30-1 Oyaguchi-kamicho, Itabashi-ku, Tokyo, Japan*
[c] *Department of Virology, Division of Medical Science, Medical Research Institute, Tokyo Medical and Dental University, 1-5-45 Yushima, Bunkyo-ku, Tokyo 113-8519, Japan*

Received 29 May 2007; received in revised form 7 September 2007; accepted 7 September 2007
Available online 25 October 2007

Abstract

The Epstein-Barr virus (EBV)-encoded oncoprotein latent membrane protein 1 (LMP1) has an essential role in B-lymphocyte transformation by the virus and is expressed in certain EBV-associated tumors and lymphoproliferative disorders. By using the Flp-In/TREx-inducible expression system, we introduced LMP1 into two human cell lines, Jurkat and HEK-293, and found that in both of them the putative cellular oncogene *Bcl*-3 is rapidly induced following the expression of LMP1. Bcl-3 was also induced in Ramos cells after in vitro EBV infection and after transfection with an LMP1 expression vector. This LMP1-induced Bcl-3 expression is considered to be mediated by the transcription factor NF-κB, because (1) deletion of a critical NF-κB-binding site in the Bcl-3 promoter abolished its responsiveness to LMP1, (2) an IκB mutant that specifically inhibits NF-κB activity suppressed the LMP1-induced activation of the Bcl-3 promoter, and (3) an LMP1 mutant lacking its effector domain CTAR2, required for the activation of NF-κB, is severely impaired in its ability to induce Bcl-3. Western blot analyses showed that all EBV-infected and LMP1-expressing lymphoid cell lines express Bcl-3. These results suggest the possibility that Bcl-3 is involved in the pathogenesis of certain EBV-associated malignancies and lymphoproliferative disorders.

Keywords: Epstein-Barr virus; LMP1; Bcl-3; NF-κB

1. Introduction

Epstein-Barr virus (EBV), a member of the genus *Lymphocryptovirus* of the family *Herpesviridae*, is a tumor virus involved in the pathogenesis of human tumors, such as Burkitt's lymphoma (BL), nasopharyngeal carcinoma (NPC), Hodgkin's disease (HD), peripheral T-cell lymphoma, gastric carcinoma, and post-transplantation lymphoproliferative disease (Rickinson and Kieff, 2001). Consistent with its nature as a tumor virus, EBV has the ability to transform human B lymphocytes and establish a lymphoblastoid cell line (LCL) that can proliferate indefinitely in culture (Kieff and Rickinson, 2001). In LCLs, EBV persists as circular episomes and expresses six nuclear proteins (EBNAs 1, 2, 3A, 3B, 3C, and LP), three membrane proteins (LMPs 1, 2A, and 2B), and two untranslated small RNAs (EBERs 1 and 2). In addition, a series of extensively spliced mRNAs are transcribed from the BamHI-A region, but their translation in the virus-infected cells has not been clearly demonstrated (Kieff and Rickinson, 2001). This type of viral gene expression, typically seen in LCLs, is designated as latency III. In EBV-associated tumors, some or all of these latency III genes are expressed and considered

* Corresponding author. Tel.: +81 3 3417 2457; fax: +81 3 3417 2419.
E-mail address: shige@nch.go.jp (S. Fujiwara).

0168-1702/$ – see front matter © 2007 Elsevier B.V. All rights reserved.
doi:10.1016/j.virusres.2007.09.003

to play critical roles in tumorigenesis (Rickinson and Kieff, 2001).

LMP1 plays an essential role in the EBV-induced transformation of B cells and has the ability to transform rodent fibroblasts (Cahir-McFarland and Kieff, 2005). It is a transmembrane protein composed of the amino-terminal cytoplasmic region, six transmembrane domains, and the carboxy-terminal cytoplasmic region. LMP1 functions as a constitutively activated receptor (Gires et al., 1997) and transmits signals through interaction with the tumor necrosis factor (TNF) receptor-associated factors (TRAFs) (Devergne et al., 1996; Mosialos et al., 1995), the TNF receptor-associated death domain protein (TRADD) (Eliopoulos et al., 1999a; Izumi et al., 1999), and the Janus kinase 3 (Gires et al., 1999). Consequent to these interactions and activation of signaling pathways, transcription factors such as NF-κB, AP-1, ATF-2 and STAT1 are activated (Devergne et al., 1996; Eliopoulos et al., 1999b; Eliopoulos and Young, 1998; Gires et al., 1999; Izumi et al., 1999; Kieser et al., 1997). LMP1 is expressed in certain EBV-associated tumors, including HD, NPC, and peripheral T-cell lymphoma, with the latency II program (EBNA1$^+$, EBNA2$^-$, and LMP1$^+$) of EBV gene expression, and plays crucial roles in the generation of tumor cell phenotypes by inducing the expression of cytokines, chemokines, growth factors, anti-apoptotic proteins, adhesion molecules, etc. (Gires et al., 1997; Hatzivassiliou et al., 1998; Herbst et al., 1996; Kilger et al., 1998; Knecht et al., 1996; Rickinson and Kieff, 2001; Zimber-Strobl et al., 1996). LMP1 is also expressed in the virus-infected T or NK cells that proliferate in T/NK lymphoproliferative diseases, such as chronic active EBV infection (CAEBV) (Yoshioka et al., 2001), nasal NK/T-cell lymphoma (Harabuchi et al., 1990), and EBV-associated hemophagocytic lymphohistiocytosis (Yoshioka et al., 2003).

Because the latency II program of EBV gene expression is associated with T-cell tumors and lymphoproliferation such as peripheral T-cell lymphoma and CAEBV, and epithelial cancers such as NPC, we intended to investigate the effect of LMP1 expression on the gene expression in these cell types. LMP1 gene was introduced in the human Jurkat (T-cell) and HEK-293 (epithelial) cell lines by using the Flp-In/TREx-inducible expression system. Experiments with these cells revealed that expression of the putative oncogene *Bcl-3* is rapidly induced following the expression of LMP1 in a NF-κB-dependent manner. Bcl-3 was also shown induced in Ramos cells that were infected with EBV in vitro or transfected with an LMP1 expression vector. Since Bcl-3 is known to be involved in the control of survival and proliferation of lymphocytes, and it is supposed to have crucial roles in the genesis of certain lymphoid malignancies, we presume that the LMP1-induced Bcl-3 is an important effector in the pathogenesis of certain EBV-associated malignancies and lymphoproliferative diseases.

2. Materials and methods

2.1. Cells

Jurkat, MOLT-4F, MOLT-14, and PEER are human leukemic T-cell lines. Raji is an EBV-positive BL cell line that expresses LMP1. Ramos, Loukes, and BL-2 are EBV-negative BL lines, and BJAB is a non-BL B-lymphoma line. LCL/95/1 through LCL/95/4 are human lymphoblastoid cell lines established by the B95-8 EBV. LCL/Sp/1 and LCL/Sp/2 are EBV-positive LCLs spontaneously established from the peripheral blood of EBV-seropositive donors. KHYG-1 is a human natural killer cell line. B95-8 is an EBV-infected lymphoblastoid cell line (LCL) of a cotton-top tamarin (*Saguinus oedipus*) origin, and produces a prototype strain of EBV. These cell lines were grown in RPMI 1640 (Sigma–Aldrich, St. Louis, MO) supplemented with 10% fetal bovine serum (FBS), penicillin (100 U/ml), and streptomycin (100 μg/ml) at 37 °C in 5% CO_2 atmosphere. SNT8, SNT13, SNT15, SNT16, and SNT20 are EBV-infected T-cell lines derived from either CAEBV or nasal NK/T-cell lymphoma (Nagata et al., 2001; Oyoshi et al., 2003; Zhang et al., 2003). SNK6 and SNK10 are EBV-infected NK-cell lines derived from nasal NK/T-cell lymphoma (Nagata et al., 2001; Zhang et al., 2003). These EBV-infected T- and NK-cell lines were cultured in the medium supplemented with IL-2 (700 U/ml) and human serum instead of FBS. HEK-293 is a human epithelial cell line derived from embryonic kidney and was cultured in Dulbecco's Modified Eagle's Medium (Sigma–Aldrich) supplemented with 10% FBS, penicillin (100 U/ml), and streptomycin (100 mg/ml).

2.2. The Flp-In/TREx expression system

The Flp-In Jurkat cells, which contain a Flp recombination target (FRT) site and a lacZ-Zeocin fusion gene, were obtained from Invitrogen (Carlsbad, CA). To develop a doxycycline (Dox)-inducible expression system in Jurkat cells, the Flp-In/TREx Jurkat cells constitutively expressing the tetracycline repressor were established by introducing pcDNA6/TR (Invitrogen) into the Flp-In Jurkat cells. The Flp-In/TREx Jurkat-LMP1 cells in which expression of LMP1 is induced by Dox were generated as described previously (Nakamura et al., 2003). Briefly, a FLAG-tagged LMP1 was generated by PCR using a forward primer 5′-CGCGATATCGCCGCCACCATGGACTACAAAGACCATGACGGTGATTACAAGGATGACGATGACAAGGAACACGACCTTGAGAGGGGCCCACCG-3′ (EcoRV site is underlined and FLAG sequence double-underlined), and a reverse primer 5′-CGCGGATCCTTAGTCATAGTAGCTTAGCTGAAC-3′ (BamHI site underlined). pSG5-LMP1 (Kaykas et al., 2002), kindly provided by Bill Sugden, was used as template. The PCR product was cloned into the pcDNA5/FRT/TO TOPO vector (Invitrogen) using the pcDNA5/FRT/TO TOPO TA expression kit (Invitrogen), to yield pcDNA5/FRT/TO-FLAG-LMP1. pcDNA/FRT/TO-FLAG-LMP1 and pOG44 (Invitrogen) were cotransfected at a ratio of 1:9 (w/w) into Flp-In/TREx Jurkat cells by electroporation, and cells resistant to hygromycin B (Wako Chemical, Osaka, Japan) (1 mg/ml) was selected. Selected cells were then confirmed for the Dox (BD Biosciences Clontech, Palo Alto, CA)-induced LMP1 expression, and designated Flp-In/TREx Jurkat-LMP1. The Flp-In/TREx 293-LMP1 cells were prepared just as the Flp-In/TREx Jurkat-LMP1 cells, except that the FLAG sequence was not included and the human epithelial cell line HEK-293 was used.

For constitutive LMP1 expression by stable transfection of Ramos cells, an LMP1 expression vector (pHN-LMP1) previously described was used (Takanashi et al., 1999).

2.3. LMP1 mutants

FLAG-tagged LMP1 and its deletion mutants were generated by PCR using pSG5-LMP1 as template. LMP1 (wild type (wt)) was produced with a common forward primer 5′-CGC AAGCTTGAACACGACCTTGAGAGGGGCCCACCG-3′ (HindIII site underlined) and a reverse primer 5′-CGCGGATCC-TTAGTCATAGTAGCTTAGCTGAAC-3′ (BamHI site underlined). LMP1 (Δ332–386) with deletion of amino acids (aas) 332–386 was generated with the common forward primer and a reverse primer 5′-CGCGGATCCTTATCCTTTGTTTTCAAC-CTCTTCCG-3′ (BamHI site underlined). LMP1 (Δ187–386) with deletion of aas 187–386 was generated with the common forward primer and a reverse primer 5′-CGCGGATCCTTAGTAATACATCCAGATTAAAATCG-3′ (BamHI site underlined). Each PCR product was digested with HindIII and BamHI and cloned into p3xFLAG-CMV10 (Sigma–Aldrich).

2.4. Reporter plasmids and luciferase assay

The human Bcl-3 promoter was amplified by PCR using genomic DNA isolated from the BJAB cells as template. The full-length Bcl-3 promoter P1 was amplified with a forward primer 5′-CGCCTCGAGATGTCTCTTTCTCTCTG-TGCACC-3′ (XhoI site underlined) and a common reverse primer 5′-CGCAAGCTTACGGCGGCCGGAGAGCGGCTG-3′ (HindIII site underlined), and covers the nucleotide −896 to +70 relative the transcription initiation site described by Ohno et al. (1990). Mutant Bcl-3 promoters were amplified with the common reverse primer at +70 and the following forward primers; 5′-CGCCTCGAGGCACCCACCCCGGTGCCCCGCG-3′ (XhoI site underlined) at −860 (P2), 5′-CGCGAGCTCAGGC-CTGGCTGCCCCAG-3′ (SacI site underlined) at −215 (P3), 5′-CGCGAGCTCCGTACGGGTGGCCCCGG-3′ (SacI site underlined) at −91 (P4), and 5′-CGCGAGCTCGGCGC-CCGGCGAAACCACCC-3′ (SacI site underlined) at +13 (P5). These full-length and mutant promoter fragments were digested with appropriate restriction enzymes and cloned into the pGL4.17 reporter plasmid (Promega, Madison, WI). The pRc-CMV-IκBα (32A36A) (Whiteside et al., 1995) plasmid encoding a dominant negative form of IκBα (Ser32Ala, Ser36Ala) was kindly provided by Alain Israel.

Flp-In/TREx Jurkat-LMP1 cells were transfected with luciferase reporter plasmids and divided into two groups after transfection; one group was treated with Dox and the other served as negative control. Twenty-four hours after transfection, cell lysates were prepared and luciferase activity was measured. When Jurkat cells were used, the pGL4.74 Renilla luciferase reporter plasmid was included in all transfections to normalize the transfection efficiency. Cell lysates were prepared 20–24 h post-transfection, and luciferase activity was assessed using the dual luciferase reporter assay system (Promega) according to the manufacturer's instructions.

2.5. RT-PCR

RNA was extracted by using TRIzol (Invitrogen). Five micrograms of total RNA was used for the synthesis of first-strand cDNA by using oligo (dT) primers and the SuperScript III first strand synthesis system (Invitrogen) according to the manufacturer's instructions. RT-PCR was performed with the Bcl-3-specific primers, 5′-TGCTGTGGTGCAGGGTAA-CCTG-3′ (sense primer) and 5′-GCTGCCTCCTGGAGCTGG-GGAG-3′ (antisense primer), LMP1-specific primers, 5′-CGCAAGCTTGAACACGACCTTGAGAGGGGCCCACCG-3′ (sense primer, HindIII site underlined) and 5′-CGCGGATCCTTAGTCATAGTAGCTTAGCTGAAC-3′ (antisense primer, BamHI site underlined), or the β-actin-specific primers 5′-TCCTGTGGCATCCACGAAACT-3′ (sense primer) and 5′-GAAGCATTTGCGGTGGACGAT-3′ (antisense primer). Amplification reactions were run in a total volume of 50 μl for 25 cycles by using the GeneAmp PCR System 9700 thermocycler (Applied Biosystems, Foster City, CA), and then the PCR products were analyzed by 1–2% agarose gel electrophoresis.

2.6. Western blotting

Cells were lysed in sodium dodecyl sulfate (SDS) sample buffer (50 mM Tris–HCl, pH 6.8, 2% SDS, 10% glycerol, 6% 2-mercaptoethanol, 0.1% bromophenol blue), fractionated by SDS-polyacrylamide gel electrophoresis (SDS-PAGE), and transferred to the FluoroTrans W polyvinylidene difluoride membrane (PALL Corp., East Hills, NY). Membranes were blocked in TBS-T (20 mM Tris, pH 7.6, 137 mM NaCl, 0.1% Tween-20) containing 10% skim milk and then incubated with a primary antibody at appropriate dilution. Membranes were then incubated with horse radish peroxidase-conjugated goat anti-rabbit antibodies (GE Healthcare Bio-Sciences Corp., Piscataway, NJ), and antigen proteins were visualized with the enhanced chemiluminescence assay (SuperSignal; Pierce, Rockford, IL) and detected by the Fuji Phosphor Imager LAS1000 (Fujifilm, Tokyo, Japan). Polyclonal antibody to Bcl-3 (sc-185) was purchased from Santa Cruz biotechnology (Santa Cruz, CA), and antibodies against the FLAG epitopes (anti-Flag M2-HRP (A 8592)) and α-tubulin (T 5168) were obtained from Sigma–Aldrich. The LMP1-specific S12 monoclonal antibody was a kind gift from Kenzo Takada.

3. Results

3.1. Expression of LMP1 by the Flp-In/TREx system and induction of Bcl-3 by LMP1

In order to examine the function of LMP1 in the context of T cells and epithelial cells, we introduced the LMP1 gene in two human cell lines, Jurkat (T cell) and HEK-293 (epithelial), by using the Flp-In/TREx-inducible expression system.

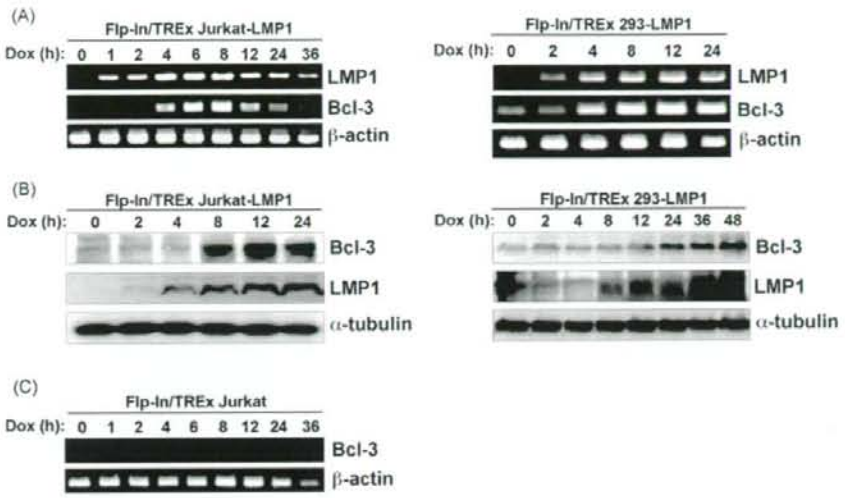

Fig. 1. Expression of LMP1 with the Flp-In/TREx system and the induction of Bcl-3 expression by LMP1. (A) Demonstration of Dox-inducible expression of LMP1 and LMP1-induced expression of Bcl-3 in the Flp-In/TREx Jurkat-LMP1 cells (left panel) and the Flp-In/TREx 293-LMP1 cells (right panel). Dox was added to culture medium and the levels of LMP1 and Bcl-3 transcripts were examined by RT-PCR at the indicated time points. Transcripts from the β-actin gene was examined as a reference. (B) Western blot detection of the Bcl-3 induction by LMP1. Dox was added to the culture medium of the Flp-In/TREx Jurkat-LMP1 cells (left panel) and the Flp-In/TREx 293-LMP1 cells (right panel) and the levels of Bcl-3 and LMP1 expression were examined by respective specific antibodies at the indicated time points. (C) The Flp-In/TREx Jurkat cells, that does not contain LMP1 gene, was examined for the expression of Bcl-3 by RT-PCR.

The stable transfectant sublines, Flp-In/TREx Jurkat-LMP1 and Flp-In/TREx 293-LMP1 were thus obtained, in which expression of LMP1 is regulated by Dox. In these cells, LMP1 mRNA was barely detectable by RT-PCR in the absence of Dox, but addition of the drug (1 μg/ml) in the culture medium resulted in its rapid induction (Fig. 1A).

Bcl-3 is a putative cellular oncogene identified in the chromosomal breakpoint of a translocation characteristic to a subgroup of chronic B-cell leukemia and has been implicated in the pathogenesis of this type of leukemia (McKeithan et al., 1987). Bcl-3 is induced in B and T lymphocytes by mitogenic stimuli (Bhatia et al., 1991; Ohno et al., 1990) suggesting that this putative oncogene is also involved in EBV-induced activation and immortalization of lymphocytes. It is also known that Bcl-3 is highly expressed in EBV-associated tumors, such as HD and NPC (Mathas et al., 2005; Thornburg et al., 2003). Since these previous findings imply the possibility that Bcl-3 is involved in lymphocyte immortalization and malignant transformation of cells by EBV, we examined whether LMP1, a key molecule in EBV-induced immortalization and malignant transformation, has an influence on the expression of Bcl-3. We utilized the Flp-In/TREx Jurkat-LMP1 and Flp-In/TREx 293-LMP1 cells and compared the level of Bcl-3 expression before and after the Dox-induced expression of LMP1. In the Flp-In/TREx Jurkat-LMP1 cells, Bcl-3 mRNA was undetectable without Dox but could be detected at 4 h after the addition of Dox, reached a peak level at 8 h, and thereafter gradually disappeared. In the Flp-In/TREx 293-LMP1 cells, on the other hand, Bcl-3 mRNA was weakly detectable without Dox but its expression was significantly up-regulated by Dox (Fig. 1A). This LMP1-induced expression of Bcl-3 was confirmed at the protein level by immunoblot analysis. The Bcl-3 protein was first visible at 8 h and reached a peak level at 12 h in the Flp-In/TREx Jurkat-LMP1 cells. In the Flp-In/TREx 293-LMP1 cells, on the other hand, low level Bcl-3 protein was detected without Dox but its level was significantly up-regulated by the drug (Fig. 1B). The induction of LMP1 protein expression by Dox occurred more slowly in Flp-In/TREx 293-LMP1 cells than in Flp-In/TREx Jurkat-LMP1 cells, and consequently Bcl-3 protein was also up-regulated more slowly in the former. Treatment of the Flp-In/TREx Jurkat and Flp-In/TREx 293 cells with Dox, in which the tetracycline repressor is consistently expressed but no LMP1 gene was introduced, did not induce the expression of Bcl-3 as assessed by RT-PCR (Fig. 1C and data not shown).

3.2. Promoter of the Bcl-3 gene is activated by LMP1 through NF-κB

To test if the induced expression of Bcl-3 mRNA and protein is due to transcriptional activation of the Bcl-3 promoter, luciferase reporter assay was performed. The promoter region (−896/+70 relative to the transcriptional initiation site reported by Ohno et al., 1990) of the *Bcl-3* gene was amplified by PCR and cloned into the luciferase reporter plasmid pGL4.17 (Fig. 2A). This plasmid (P1) was introduced in the Flp-In/TREx Jurkat-LMP1 cells by electroporation and the expression of LMP1 was induced by Dox. The cells were then lysed and measured for luciferase activity. The results are shown in Fig. 2B and indicated that the Bcl-3 promoter activity was up-regulated about three times by addition of Dox. Thus, the induction of Bcl-3 by LMP1 could be at least partially explained by transcriptional activation of its promoter.

According to the previous report by Ohno et al. (1990) and the cDNA catalogue published in the Database of Transcriptional

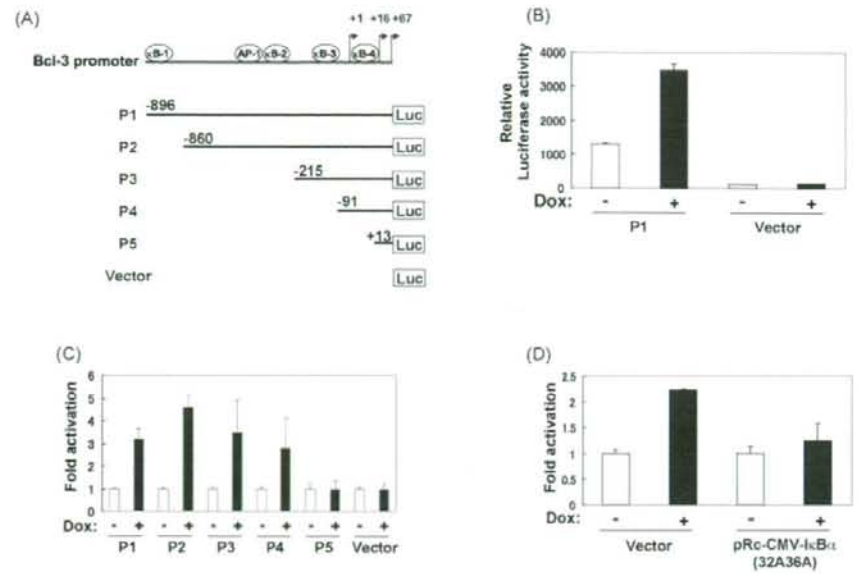

Fig. 2. Activation of the Bcl-3 promoter and its deletion mutants by LMP1. (A) Schematic presentation of the Bcl-3 promoter and the structures of the luciferase reporter constructs containing various parts of the promoter. The transcription initiation site reported by Ohno et al. (1990) was assigned number +1 and each nucleotides are numbered relative to it. The two initiation sites (located at +16 and +67) published in DBTSS are also shown. Previously reported (Brasier et al., 2001; Nolan et al., 1993) consensus binding motifs for NF-κB (κB-1–κB-4) and AP-1 are indicated. The luciferase reporter plasmid containing the full-length Bcl-3 promoter (designated P1) and those containing various deletion mutants of the promoter (designated P2–P5) are shown with their respective 5′ endpoints. (B) Bcl-3 promoter activation by LMP1. Flp-In/TREx Jurkat-LMP1 cells were transfected with P1 or an empty vector and incubated with (+) or without (−) Dox for 24 hr and examined for luciferase activity. (C) Analyses of deletion mutants of the Bcl-3 promoter. Flp-In/TREx Jurkat-LMP1 cells were transfected with P1, one of the deletion mutants P2–P5, or an empty vector, and incubated with or without Dox for 24 h. Fold activation by Dox is shown to control for the differences in basal activities of each construct. (D) Effect of an IκBα mutant. Flp-In/TREx Jurkat-LMP1 cells were transfected with either pRc-CMV-IκBα (32A36A) (encoding an IκBα mutant) or empty vector and incubated with or without Dox for 24 h. Fold activation of luciferase activity by Dox is shown. In the luciferase assays shown in B–D, triplicate samples were examined and the data shown represent the mean and the standard error of the mean. Each experiment was repeated three times and a representative result is shown.

Start Sites (DBTSS) (http://dbtss.hgc.jp/), three transcriptional initiation sites (+1, +16, and +67, with the site described by Ohno et al. being assigned +1) have been identified in the Bcl-3 promoter. Nolan et al. (1993) described two binding sites for NF-κB (κB-2 and κB-4 in Fig. 2A) in the promoter region of the human *Bcl*-3 gene, while Brasier et al. (2001) identified two other NF-κB-binding sites (κB-1 and κB-3) and an AP-1-binding site in this promoter (Fig. 2A). Based on these findings, we prepared four 5′ deletion mutants of the Bcl-3 promoter, P2–P5, to analyze the contribution of these binding sites in the LMP1-induced Bcl-3 expression. The structure of these promoter mutants, with locations of binding sites for transcription factors, are schematically presented in Fig. 2A. The results of luciferase assay using these deletion mutants are shown in Fig. 2C. The ratio of luciferase activity in the presence and absence of Dox (i.e. fold activation by LMP1) remained largely unchanged in P1–P4, although a relatively high fold activation was found in P2. These results suggest that κB-1, κB-2, κB-3, and the AP-1 sites do not have major roles in the LMP1-induced expression of Bcl-3. In contrast, when κB-4 was deleted (P5), activation of the promoter by LMP1 was totally lost, suggesting that the κB-4 site has a predominant role in the LMP1-induced activation of the Bcl-3 promoter.

Since the results described above suggested that the LMP1-induced expression of Bcl-3 in Jurkat cells is mediated by activation of NF-κB, we examined the effect of an IκB mutant that cannot be phosphorylated and hence inhibits activation of NF-κB. The Flp-In/TREx Jurkat-LMP1 cells were transfected with pRc-CMV-IκBα (32A36A) (Whiteside et al., 1995) encoding a dominant negative mutant of IκBα (Ser32Ala, Ser36Ala) together with the luciferase reporter plasmid P1 containing the full-length Bcl-3 promoter, and incubated with or without Dox for 24 h. Cells were then lysed and examined for luciferase activity. The result is shown in Fig. 2D and indicated that activation of the Bcl-3 promoter by LMP1 is suppressed by the IκBα mutant, confirming the involvement of NF-κB in the LMP1-induced Bcl-3 induction.

3.3. The LMP1 effector domain CTAR2 is important for the activation of the Bcl-3 promoter

LMP1 has two effector domains, CTAR1 and CTAR2, in its carboxyl-terminal cytoplasmic region (Fig. 3A). CTAR1 recruits TRAF-1, -2, -3, and -5, and initiates the non-canonical pathway of NF-κB activation, whereas CTAR2 engages RIP and TRADD, and triggers the canonical pathway (Cahir-McFarland and Kieff, 2005). In order to analyze the contributions of these

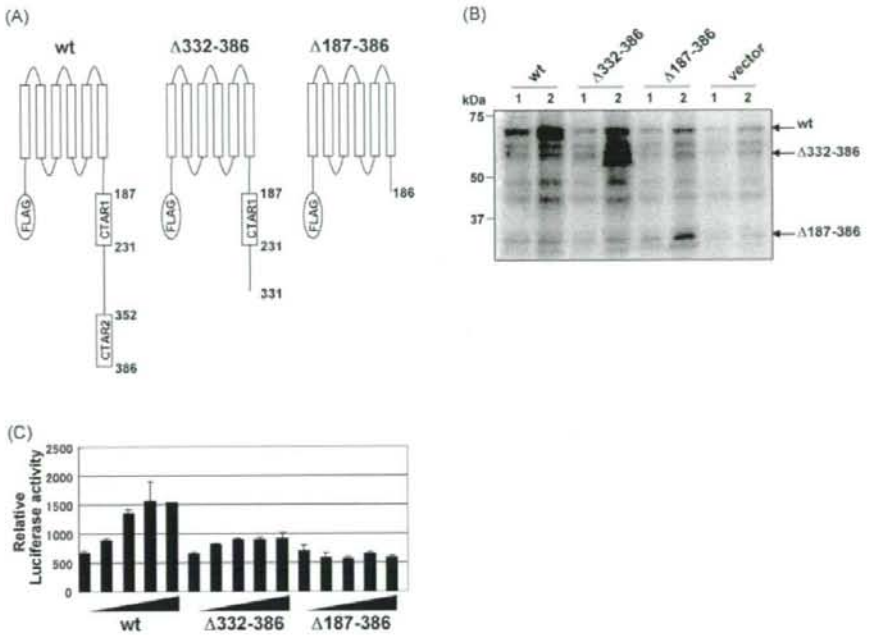

Fig. 3. Transactivation of the Bcl-3 promoter by LMP1 and its deletion mutants. (A) Schematic representations of the LMP1 construct and its deletion mutants. The wild-type (wt) LMP1 is composed of the amino-terminal cytoplasmic region, six transmembrane segments, and the carboxy-terminal cytoplasmic region containing the CTAR1 and CTAR2 effector domains. The FLAG epitope was conjugated to the N terminus to facilitate detection by antibody. The LMP1 mutant LMP1 (Δ332–386) is deleted for the amio acid residues 332–386 and hence lacks CTAR2. The LMP1 mutant LMP1 (Δ187–386) is deleted for the amino acid residues 187–386 and lacks both CTAR1 and CTAR2. (B) Western blot analysis of the LMP1 mutants. 2.5 μg (lane 1) or 7.5 μg (lane 2) of the expression vectors for LMP1 (wt), LMP1 (Δ332–386) and LMP1 (Δ187–386), as well as empty vector, were transiently transfected into Jurkat cells and the cell lysate was examined by Western blotting with the antibody to the FLAG epitope. (C) Luciferase assay. Increasing amounts (0, 1, 2.5, 5, 7.5 μg) of the expression constructs for LMP1 (wt), LMP1 (Δ332–386), or LMP1 (Δ187–386) were transfected to Jurkat cells together with the luciferase reporter plasmid containing the full-length Bcl-3 promoter, and after 24 h of culture, cells were harvested and examined for luciferase activity. Triplicate samples were examined and the data shown represent the mean and the standard error of the mean. Each experiment was repeated three times and a representative result is shown.

LMP1 effector domains in the induction of Bcl-3, we prepared LMP1 deletion mutants (Fig. 3A and B) and introduced them, together with a luciferase reporter plasmid containing the full-length Bcl-3 promoter (P1), into Jurkat cells by electroporation. When LMP1 (wt) was introduced in Jurkat cells, luciferase activity increased in a dose-dependent manner (Fig. 3C). The mutant LMP1 (Δ332–386) that lacks CTAR2, in contrast, activated the luciferase reporter gene only very slightly (Fig. 3C). LMP1 (Δ187–386) that lacks both CTAR1 and CTAR2 did not induce the reporter gene even at the highest dose examined (Fig. 3C). These results suggest that the canonical pathway of NF-κB activation, initiated by CTAR2, is primarily important in the LMP1-induced activation of the Bcl-3 promoter, although some contribution from CTAR1 could not be ruled out.

3.4. Expression of Bcl-3 in EBV-infected and -uninfected lymphoid cell lines

In order to extend our finding of Bcl-3 induction by LMP1 obtained by gene transfer experiments, we examined various EBV-infected and -uninfected lymphoid cell lines for the expression of Bcl-3 (Fig. 4A and B). Fourteen T-cell lines were examined, among which seven were EBV-positive and the other seven EBV-negative, and all EBV-positive lines were shown to express modest to high levels of Bcl-3 (Fig. 4A). EBV-negative T-cell lines, in contrast, did not express significant levels of Bcl-3, except for HUT-78, in which high level of the protein was detected. Among the 11 B-cell lines examined, 7 of which was EBV-positive and the other 4 were the virus-negative, modest to high levels of Bcl-3 was detected in each cell line (Fig. 4B). The EBV-negative BL cells Ramos express only a marginal level of Bcl-3, but following expression of LMP1 by gene transfer or in vitro infection of EBV, significant levels of Bcl-3 expression was induced (Fig. 4C and D). Bcl-3 expression was also examined by RT-PCR in peripheral blood B cells and relatively high levels of transcripts could be detected, and this level was not altered significantly after in vitro EBV infection (data not shown). The data described above imply that in B-cells, expression of Bcl-3 is common irrespective of the presence of EBV, whereas in T-cells, Bcl-3 expression correlates with infection with EBV. Thus, choice of non B-cell lines as the recipient of LMP1 gene transfer may have facilitated the identification of Bcl-3 as an LMP1-inducible gene. It should be noted that HUT-78, the only

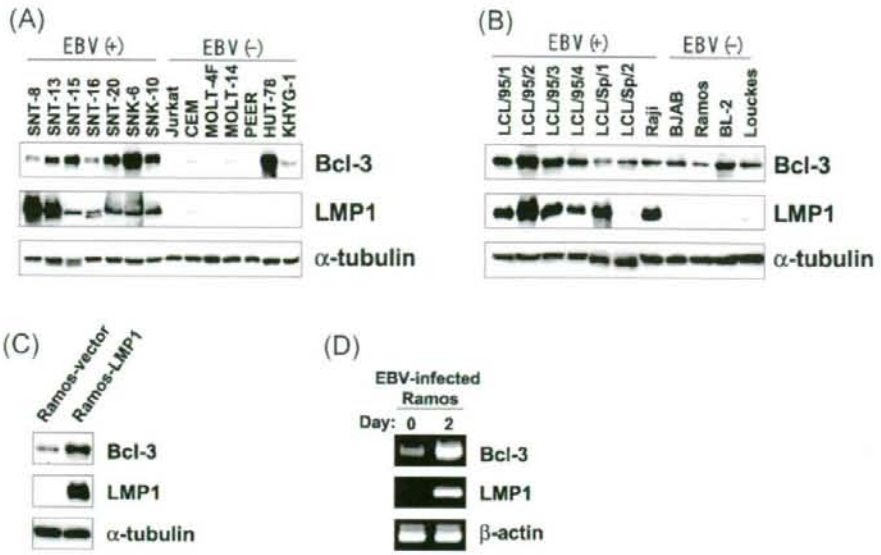

Fig. 4. Expression of Bcl-3 in EBV-infected and uninfected cell lines. (A) Western blot detection of Bcl-3 and LMP1 in the EBV-infected and -uninfected T-cell lines. The name of each cell line and its EBV status are shown on top of each lane. α-Tubulin was examined as a reference. (B) Western blot detection of Bcl-3 and LMP1 in the EBV-infected and -uninfected B-cell lines. The name of each cell line and its EBV status are shown on top of each lane. α-Tubulin was examined as a reference. (C) Up-regulation of Bcl-3 expression in Ramos cells by transfection of the LMP1 gene. Ramos cells were stably transfected with the LMP1 expression vector pHN-LMP or an empty vector, and the Bcl-3 protein was detected by Western blotting. LMP1 and α-tubulin were examined as references. (D) Up-regulation of Bcl-3 expression in Ramos cells by in vitro infection with EBV. Ramos cells were infected in vitro with the B95-8 EBV and examined for Bcl-3 transcripts by RT-PCR. Transcripts for LMP1 and β-actin were examined as references.

EBV-negative T-cell line shown here to express high level Bcl-3, has been reported to have constitutively high NF-κB activity (Giri and Aggarwal, 1998).

4. Discussion

In this manuscript, we presented evidence that EBV-encoded LMP1 induces the expression of the putative oncogene *Bcl-3* through its transcriptional activation. This finding was first made in the human T-cell line Jurkat and epithelial cell line HEK-293 in which LMP1 was inducibly expressed by using the Flp-In/TREx expression system. Induction of Bcl-3 was also demonstrated in the EBV-negative BL cells Ramos that were either in vitro infected with EBV or transfected with an LMP1 expression vector, indicating that this LMP1-induced expression of Bcl-3 occurs also in B cells. Consistent with these findings, all EBV-infected and LMP1-expressing human T- and B-cell lines examined in this study were found to express modest to high levels of Bcl-3. The LMP1-induced Bcl-3 expression is considered to be mediated by the transcription factor NF-κB, because (1) deletion of a critical NF-κB site in the Bcl-3 promoter abolished its responsiveness to LMP1, (2) an IκB mutant that specifically inhibits NF-κB suppressed the LMP1-induced activation of the Bcl-3 promoter, and (3) an LMP1 mutant lacking its effector domain CTAR2, required for the activation of NF-κB, barely induced Bcl-3.

The regulation of the *Bcl-3* gene expression at the transcription level has not been characterized in detail. Brasier et al. (2001) examined the function of two NF-κB-binding sites (corresponding to the κB-1 and κB-3 in this study) and reported that κB-3 plays an essential role in the RelA-induced activation of the promoter, whereas the function of κB-2 and κB-4 has not been characterized well. The present study indicated that κB-4 plays an important role in the LMP1-induced activation of the Bcl-3 promoter. It was also shown here that the AP-1-binding site in the promoter does not play a significant role in this process.

The proto-oncogene *Bcl-3* was initially identified as a gene located next to the breakpoint junction of the t(14;19) translocation characteristic to a subtype of chronic B-cell leukemia (McKeithan et al., 1987). As a consequence of this translocation, the transcription of Bcl-3 is up-regulated (McKeithan et al., 1997; Ohno et al., 1993), and the elevated level of Bcl-3 expression is supposed to have an important role in oncogenesis. Bcl-3 has been also implicated in other human malignancies, including breast cancer (Cogswell et al., 2000) and tumors of hair follicle keratinocytes (Massoumi et al., 2006). Bcl-3 contains ankyrin repeats that interact with the Rel domain of NF-κB family proteins and hence categorized in the IκB family (Franzoso et al., 1992; Wulczyn et al., 1992). Similar to other IκB proteins, Bcl-3 can associate with NF-κB family proteins and functions as their antagonist (Franzoso et al., 1992; Wulczyn et al., 1992). Interestingly, however, Bcl-3 can also function as a transcriptional coactivator when bound to the homodimers of either the p50 or p52 components of the NF-κB family (Bours et al., 1993; Fujita et al., 1993; Nolan et al., 1993). Consistent with

its supposed role in certain leukemias and tumors, Bcl-3 has been reported to promote survival and proliferation of various cells, especially lymphocytes. Thus, transgenic mice expressing Bcl-3 had splenomegaly and accumulation of mature B cells in various organs, suggesting that overexpression of Bcl-3 causes B-cell proliferation (Ong et al., 1998). Bcl-3 could rescue T cells from apoptosis in various conditions (Mitchell et al., 2001; Rebollo et al., 2000; Valenzuela et al., 2005). In a human breast epithelial cell line, Bcl-3 could induce the expression of cyclin D1 and stimulate G1 transition (Westerheide et al., 2001). In addition, Bcl-3 expression is induced following stimulation with a variety of growth factors, including IL-9, GM-CSF, and erythropoietin (Brasier et al., 2001; Rebollo et al., 2000; Richard et al., 1999; Zhang et al., 1998). Taken together, these characteristics of Bcl-3 and the results obtained in the present study strongly suggest that it has an important role in the EBV-induced cell survival and proliferation. With respect to this point, it should be noted that all EBV-infected lymphoid cell lines examined in this study express moderate to high levels of Bcl-3, implying that the LMP1-induced expression of Bcl-3 may be a general feature of EBV-induced lymphoid proliferation.

With regard to the suggested involvement of the LMP1-induced expression of Bcl-3 in the EBV-associated tumorigenesis, two previously published papers are especially relevant. Thornburg and others reported that Bcl-3 is highly expressed and the NF-κB p50 homodimer/Bcl-3 complex is activated in NPC (Thornburg et al., 2003). Although the activation of p50 homodimer/Bcl-3 complex was found also in an NPC cell line that did not express LMP1 (Thornburg et al., 2003), the relationship between this Bcl-3 activation and the status of EBV infection (and hence expression of LMP1) should be investigated with a larger number of both EBV-positive and -negative NPC samples. It should be mentioned that the present study showed LMP1 induces the expression of Bcl-3 in both lymphoid and epithelial cells. Another interesting finding linking Bcl-3 and EBV-induced tumorigenesis and lymphoproliferation was reported by Mathas et al. (2005). They showed high-level expression of Bcl-3 and formation of the NF-κB p50 homodimer/Bcl-3 complex in classical Hodgkin's disease and anaplastic large-cell and other peripheral T-cell lymphomas. Although the relationship between the Bcl-3 expression and EBV status was not investigated in their work, it is well known that certain fractions of these tumors contain EBV genomes and express LMP1. As the results of the Western blot analyses performed in the present study with various EBV-positive and -negative lymphoid cell lines have demonstrated, Bcl-3 expression does not completely correlate with EBV status; i.e. some EBV-negative cell lines (especially B-cell lines) do express Bcl-3. However, if we suppose that elevated expression of Bcl-3 has an important role in the pathogenesis of lymphoid malignancies, this process may be triggered by LMP1 in EBV-positive cases and by some other mechanism in EBV-negative cases. Further studies will be necessary to obtain the entire picture of the involvement of Bcl-3 in the EBV-induced cell proliferation and malignant transformation.

Conflict of interest

The authors do not have a commercial and other association that might pose a conflict of interest.

Acknowledgements

We thank Kenzo Takada for providing the S12 antibody, Bill Sugden for pSG5-LMP1, and Alain Israel for pRc-CMV-IκBα (32A36A). We thank Yukari Aso for secretarial assistance.

This study was conducted with the support of a grant for Research Promotion of Emerging and Re-emerging Infectious Diseases (H18-Shinko-013) from Ministry of Health, Labour and Welfare of Japan.

References

Bhatia, K., Huppi, K., McKeithan, T., Siwarski, D., Mushinski, J.F., Magrath, I., 1991. Mouse bcl-3: cDNA structure, mapping and stage-dependent expression in B lymphocytes. Oncogene 6 (9), 1569–1573.

Bours, V., Franzoso, G., Azarenko, V., Park, S., Kanno, T., Brown, K., Siebenlist, U., 1993. The oncoprotein Bcl-3 directly transactivates through kappa B motifs via association with DNA-binding p50B homodimers. Cell 72 (5), 729–739.

Brasier, A.R., Lu, M., Hai, T., Lu, Y., Boldogh, I., 2001. NF-kappa B-inducible BCL-3 expression is an autoregulatory loop controlling nuclear p50/NF-kappa B1 residence. J. Biol. Chem. 276 (34), 32080–32093.

Cahir-McFarland, E., Kieff, E., 2005. Epstein-Barr virus latent membrane protein one. In: Robertson, E.S. (Ed.), Epstein-Barr Virus. Caister Academic Press, Norfolk, pp. 553–570.

Cogswell, P.C., Guttridge, D.C., Funkhouser, W.K., Baldwin Jr., A.S., 2000. Selective activation of NF-kappa B subunits in human breast cancer: potential roles for NF-kappa B2/p52 and for Bcl-3. Oncogene 19 (9), 1123–1131.

Devergne, O., Hatzivassiliou, E., Izumi, K.M., Kaye, K.M., Kleijnen, M.F., Kieff, E., Mosialos, G., 1996. Association of TRAF1, TRAF2, and TRAF3 with an Epstein-Barr virus LMP1 domain important for B-lymphocyte transformation: role in NF-kappaB activation. Mol. Cell Biol. 16 (12), 7098–7108.

Eliopoulos, A.G., Blake, S.M., Floettmann, J.E., Rowe, M., Young, L.S., 1999a. Epstein-Barr virus-encoded latent membrane protein 1 activates the JNK pathway through its extreme C terminus via a mechanism involving TRADD and TRAF2. J. Virol. 73 (2), 1023–1035.

Eliopoulos, A.G., Gallagher, N.J., Blake, S.M., Dawson, C.W., Young, L.S., 1999b. Activation of the p38 mitogen-activated protein kinase pathway by Epstein-Barr virus-encoded latent membrane protein 1 coregulates interleukin-6 and interleukin-8 production. J. Biol. Chem. 274 (23), 16085–16096.

Eliopoulos, A.G., Young, L.S., 1998. Activation of the cJun N-terminal kinase (JNK) pathway by the Epstein-Barr virus-encoded latent membrane protein 1 (LMP1). Oncogene 16 (13), 1731–1742.

Franzoso, G., Bours, V., Park, S., Tomita-Yamaguchi, M., Kelly, K., Siebenlist, U., 1992. The candidate oncoprotein Bcl-3 is an antagonist of p50/NF-kappa B-mediated inhibition. Nature 359 (6393), 339–342.

Fujita, T., Nolan, G.P., Liou, H.C., Scott, M.L., Baltimore, D., 1993. The candidate proto-oncogene bcl-3 encodes a transcriptional coactivator that activates through NF-kappa B p50 homodimers. Genes Dev. 7 (7B), 1354–1363.

Gires, O., Kohlhuber, F., Kilger, E., Baumann, M., Kieser, A., Kaiser, C., Zeidler, R., Scheffer, B., Ueffing, M., Hammerschmidt, W., 1999. Latent membrane protein 1 of Epstein-Barr virus interacts with JAK3 and activates STAT proteins. EMBO J. 18 (11), 3064–3073.

Gires, O., Zimber-Strobl, U., Gonnella, R., Ueffing, M., Marschall, G., Zeidler, R., Pich, D., Hammerschmidt, W., 1997. Latent membrane protein 1 of

Epstein-Barr virus mimics a constitutively active receptor molecule. EMBO J. 16 (20), 6131–6140.

Giri, D.K., Aggarwal, B.B., 1998. Constitutive activation of NF-kappaB causes resistance to apoptosis in human cutaneous T cell lymphoma HuT-78 cells. Autocrine role of tumor necrosis factor and reactive oxygen intermediates. J. Biol. Chem. 273 (22), 14008–14014.

Harabuchi, Y., Yamanaka, N., Kataura, A., Imai, S., Kinoshita, T., Mizuno, F., Osato, T., 1990. Epstein-Barr virus in nasal T-cell lymphomas in patients with lethal midline granuloma. Lancet 335 (8682), 128–130.

Hatzivassiliou, E., Miller, W.E., Raab-Traub, N., Kieff, E., Mosialos, G., 1998. A fusion of the EBV latent membrane protein-1 (LMP1) transmembrane domains to the CD40 cytoplasmic domain is similar to LMP1 in constitutive activation of epidermal growth factor receptor expression, nuclear factor-kappa B, and stress-activated protein kinase. J. Immunol. 160 (3), 1116–1121.

Herbst, H., Raff, T., Stein, H., 1996. Phenotypic modulation of Hodgkin and Reed-Sternberg cells by Epstein-Barr virus. J. Pathol. 179 (1), 54–59.

Izumi, K.M., Cahir McFarland, E.D., Ting, A.T., Riley, E.A., Seed, B., Kieff, E.D., 1999. The Epstein-Barr virus oncoprotein latent membrane protein 1 engages the tumor necrosis factor receptor-associated proteins TRADD and receptor-interacting protein (RIP) but does not induce apoptosis or require RIP for NF-kappaB activation. Mol. Cell Biol. 19 (8), 5759–5767.

Kaykas, A., Worringer, K., Sugden, B., 2002. LMP-1's transmembrane domains encode multiple functions required for LMP-1's efficient signaling. J. Virol. 76 (22), 11551–11560.

Kieff, E., Rickinson, A.B., 2001. Epstein-Barr virus and its replication. In: Knipe, D.M., Howley, P.M. (Eds.), Fields Virology, 4th ed. Lippincott Williams & Wilkins, Philadelphia, pp. 2511–2574.

Kieser, A., Kilger, E., Gires, O., Ueffing, M., Kolch, W., Hammerschmidt, W., 1997. Epstein-Barr virus latent membrane protein-1 triggers AP-1 activity via the c-Jun N-terminal kinase cascade. EMBO J. 16 (21), 6478–6485.

Kilger, E., Kieser, A., Baumann, M., Hammerschmidt, W., 1998. Epstein-Barr virus-mediated B-cell proliferation is dependent upon latent membrane protein 1, which simulates an activated CD40 receptor. EMBO J. 17 (6), 1700–1709.

Knecht, H., McQuain, C., Martin, J., Rothenberger, S., Drexler, H.G., Berger, C., Bachmann, E., Kittler, E.L., Odermatt, B.F., Quesenberry, P.J., 1996. Expression of the LMP1 oncoprotein in the EBV negative Hodgkin's disease cell line L-428 is associated with Reed-Sternberg cell morphology. Oncogene 13 (5), 947–953.

Massoumi, R., Chmielarska, K., Hennecke, K., Pfeifer, A., Fassler, R., 2006. Cyld inhibits tumor cell proliferation by blocking Bcl-3-dependent NF-kappaB signaling. Cell 125 (4), 665–677.

Mathas, S., Johrens, K., Joos, S., Lietz, A., Hummel, F., Janz, M., Jundt, F., Anagnostopoulos, I., Bommert, K., Lichter, P., Stein, H., Scheidereit, C., Dorken, B., 2005. Elevated NF-kappaB p50 complex formation and Bcl-3 expression in classical Hodgkin, anaplastic large-cell, and other peripheral T-cell lymphomas. Blood 106 (13), 4287–4293.

McKeithan, T.W., Rowley, J.D., Shows, T.B., Diaz, M.O., 1987. Cloning of the chromosome translocation breakpoint junction of the t(14;19) in chronic lymphocytic leukaemia. Proc. Natl. Acad. Sci. U.S.A. 84 (24), 9257–9260.

McKeithan, T.W., Takimoto, G.S., Ohno, H., Bjorling, V.S., Morgan, R., Hecht, B.K., Dube, I., Sandberg, A.A., Rowley, J.D., 1997. BCL3 rearrangements and t(14;19) in chronic lymphocytic leukemia and other B-cell malignancies: a molecular and cytogenetic study. Genes Chromosomes Cancer 20 (1), 64–72.

Mitchell, T.C., Hildeman, D., Kedl, R.M., Teague, T.K., Schaefer, B.C., White, J., Zhu, Y., Kappler, J., Marrack, P., 2001. Immunological adjuvants promote activated T cell survival via induction of Bcl-3. Nat. Immunol. 2 (5), 397–402.

Mosialos, G., Birkenbach, M., Yalamanchili, R., VanArsdale, T., Ware, C., Kieff, E., 1995. The Epstein-Barr virus transforming protein LMP1 engages signaling proteins for the tumor necrosis factor receptor family. Cell 80 (3), 389–399.

Nagata, H., Konno, A., Kimura, N., Zhang, Y., Kimura, M., Demachi, A., Sekine, T., Yamamoto, K., Shimizu, N., 2001. Characterization of novel natural killer (NK)-cell and gammadelta T-cell lines established from primary lesions of nasal T/NK-cell lymphomas associated with the Epstein-Barr virus. Blood 97 (3), 708–713.

Nakamura, H., Lu, M., Gwack, Y., Souvlis, J., Zeichner, S.L., Jung, J.U., 2003. Global changes in Kaposi's sarcoma-associated virus gene expression patterns following expression of a tetracycline-inducible Rta transactivator. J. Virol. 77 (7), 4205–4220.

Nolan, G.P., Fujita, T., Bhatia, K., Huppi, C., Liou, H.C., Scott, M.L., Baltimore, D., 1993. The bcl-3 proto-oncogene encodes a nuclear I kappa B-like molecule that preferentially interacts with NF-kappa B p50 and p52 in a phosphorylation-dependent manner. Mol. Cell Biol. 13 (6), 3557–3566.

Ohno, H., Doi, S., Yabumoto, K., Fukuhara, S., McKeithan, T.W., 1993. Molecular characterization of the t(14;19)(q32;q13) translocation in chronic lymphocytic leukemia. Leukemia 7 (12), 2057–2063.

Ohno, H., Takimoto, G., McKeithan, T.W., 1990. The candidate proto-oncogene bcl-3 is related to genes implicated in cell lineage determination and cell cycle control. Cell 60 (6), 991–997.

Ong, S.T., Hackbarth, M.L., Degenstein, L.C., Baunoch, D.A., Anastasi, J., McKeithan, T.W., 1998. Lymphadenopathy, splenomegaly, and altered immunoglobulin production in BCL3 transgenic mice. Oncogene 16 (18), 2333–2343.

Oyoshi, M.K., Nagata, H., Kimura, N., Zhang, Y., Demachi, A., Hara, T., Kanegane, H., Matsuo, Y., Yamaguchi, T., Morio, T., Hirano, A., Shimizu, N., Yamamoto, K., 2003. Preferential expansion of Vgamma9-JgammaP/Vdelta2-Jdelta3 gammadelta T cells in nasal T-cell lymphoma and chronic active Epstein-Barr virus infection. Am. J. Pathol. 162 (5), 1629–1638.

Rebollo, A., Dumoutier, L., Renauld, J.C., Zaballos, A., Ayllon, V., Martinez, A.C., 2000. Bcl-3 expression promotes cell survival following interleukin-4 deprivation and is controlled by AP1 and AP1-like transcription factors. Mol. Cell Biol. 20 (10), 3407–3416.

Richard, M., Louahed, J., Demoulin, J.B., Renauld, J.C., 1999. Interleukin-9 regulates NF-kappaB activity through BCL3 gene induction. Blood 93 (12), 4318–4327.

Rickinson, A.B., Kieff, E., 2001. Epstein-Barr virus. In: Knipe, D.M., Howley, P.M. (Eds.), Fields Virology. Lippincott Williams & Wilkins, Philadelphia, pp. 2575–2628.

Takanashi, M., Li, J., Shirakata, M., Mori, S., Hirai, K., 1999. Tumorigenicity of mouse BALB/c 3T3 fibroblast cells which express Epstein-Barr virus-encoded LMP1 and show normal growth phenotypes in vitro is correlated with loss of transforming growth factor-beta 1-mediated growth inhibition. Arch. Virol. 144 (2), 241–257.

Thornburg, N.J., Pathmanathan, R., Raab-Traub, N., 2003. Activation of nuclear factor-kappaB p50 homodimer/Bcl-3 complexes in nasopharyngeal carcinoma. Cancer Res. 63 (23), 8293–8301.

Valenzuela, J.O., Hammerbeck, C.D., Mescher, M.F., 2005. Cutting edge: Bcl-3 up-regulation by signal 3 cytokine (IL-12) prolongs survival of antigen-activated CD8 T cells. J. Immunol. 174 (2), 600–604.

Westerheide, S.D., Mayo, M.W., Anest, V., Hanson, J.L., Baldwin Jr., A.S., 2001. The putative oncoprotein Bcl-3 induces cyclin D1 to stimulate G(1) transition. Mol. Cell Biol. 21 (24), 8428–8436.

Whiteside, S.T., Ernst, M.K., LeBail, O., Laurent-Winter, C., Rice, N., Israel, A., 1995. N- and C-terminal sequences control degradation of MAD3/I kappa B alpha in response to inducers of NF-kappa B activity. Mol. Cell Biol. 15 (10), 5339–5345.

Wulczyn, F.G., Naumann, M., Scheidereit, C., 1992. Candidate proto-oncogene bcl-3 encodes a subunit-specific inhibitor of transcription factor NF-kappa B. Nature 358 (6387), 597–599.

Yoshioka, M., Ishiguro, N., Ishiko, H., Ma, X., Kikuta, H., Kobayashi, K., 2001. Heterogeneous, restricted patterns of Epstein-Barr virus (EBV) latent gene expression in patients with chronic active EBV infection. J. Gen. Virol. 82 (Pt 10), 2385–2392.

Yoshioka, M., Kikuta, H., Ishiguro, N., Endo, R., Kobayashi, K., 2003. Latency pattern of Epstein-Barr virus and methylation status in Epstein-Barr virus-associated hemophagocytic syndrome. J. Med. Virol. 70 (3), 410–419.

Zhang, M.Y., Harhaj, E.W., Bell, L., Sun, S.C., Miller, B.A., 1998. Bcl-3 expression and nuclear translocation are induced by granulocyte-macrophage colony-stimulating factor and erythropoietin in proliferating human erythroid precursors. Blood 92 (4), 1225–1234.

Zhang, Y., Nagata, H., Ikeuchi, T., Mukai, H., Oyoshi, M.K., Demachi, A., Morio, T., Wakiguchi, H., Kimura, N., Shimizu, N., Yamamoto, K., 2003. Common cytological and cytogenetic features of Epstein-Barr virus (EBV)-positive natural killer (NK) cells and cell lines derived from patients with nasal T/NK-cell lymphomas, chronic active EBV infection and hydroa vacciniforme-like eruptions. Br. J. Haematol. 121 (5), 805–814.

Zimber-Strobl, U., Kempkes, B., Marschall, G., Zeidler, R., Van Kooten, C., Banchereau, J., Bornkamm, G.W., Hammerschmidt, W., 1996. Epstein-Barr virus latent membrane protein (LMP1) is not sufficient to maintain proliferation of B cells but both it and activated CD40 can prolong their survival. EMBO J. 15 (24), 7070–7078.

Association of varicella zoster virus load in the aqueous humor with clinical manifestations of anterior uveitis in herpes zoster ophthalmicus and zoster sine herpete

S Kido, S Sugita, S Horie, M Miyanaga, K Miyata, N Shimizu, T Morio and M Mochizuki

Br. J. Ophthalmol. 2008;92;505-508; originally published online 1 Feb 2008; doi:10.1136/bjo.2007.125773

Association of varicella zoster virus load in the aqueous humor with clinical manifestations of anterior uveitis in herpes zoster ophthalmicus and zoster sine herpete

S Kido,[1] S Sugita,[1] S Horie,[1] M Miyanaga,[2] K Miyata,[2] N Shimizu,[3] T Morio,[4] M Mochizuki[1]

[1] Department of Ophthalmology & Visual Science, Tokyo Medical and Dental University, Tokyo, Japan; [2] Miyata Eye Hospital, Miyakonojyo, Japan; [3] Department of Virology, Medical Research Institute, Tokyo Medical and Dental University, Tokyo, Japan; [4] Center for Cell Therapy, Tokyo Medical and Dental University, Tokyo, Japan

Correspondence to: Dr S Sugita, Department of Ophthalmology & Visual Science, Tokyo Medical and Dental University Graduate School of Medicine, 1-5-45 Yushima, Bunkyo-ku, Tokyo 113-8519, Japan; sunaoph@tmd.ac.jp

Accepted 4 August 2007
Published Online First 1 February 2008

ABSTRACT

Aim: To investigative whether clinical manifestations of anterior uveitis are associated with the viral load of varicella zoster virus (VZV) in the aqueous humor in patients with herpes zoster ophthalmicus (HZO) and zoster sine herpete (ZSH).

Methods: After informed consent was given, an aliquot of aqueous humor was collected from patients with VZV anterior uveitis (n = 8). Genomic DNA of the human herpes viruses was measured in the aqueous humor by two PCR assays: a qualitative multiplex PCR and a quantitative real-time PCR.

Results: All patients had unilateral acute anterior uveitis with high intraocular pressure, mutton fat keratic precipitates with some pigmentation, and trabecular meshwork pigmentation. Multiplex PCR demonstrated VZV genomic DNA in all of the samples, but not in other human herpes virus samples (human simplex virus types 1 and 2, Epstein–Barr virus, cytomegalovirus and human herpes virus types 6, 7 and 8). Real-time PCR revealed a high copy number of VZV DNA in the aqueous humor. After the initial onset of anterior uveitis, iris atrophy and distorted pupil with paralytic mydriasis developed. The intensity of iris atrophy and pupil distortion, but not ocular hypertension, correlated with the viral load of VZV in the aqueous humor.

Conclusion: VZV viral load in the aqueous humor correlated significantly with damage to the iris (iris atrophy and pupil distortion) in patients with HZO and ZSH.

Varicella zoster virus (VZV) affects the first branch of the trigeminal nerve and is known to cause unilateral anterior uveitis (VZV anterior uveitis) characterised by mutton-fat keratic precipitates (KPs), trabecular meshwork pigmentation, ocular hypertension, iris atrophy and distorted pupil. Systemic signs in VZV iridocyclitis can be herpes zoster ophthalmicus (HZO) with skin eruptions or zoster sine herpete (ZSH) without skin eruptions but solely with neuralgia. Using PCR, previous studies have revealed genomic DNA of VZV in the aqueous humor in patients with anterior uveitis with HZO and ZSH.[1 2] Recent advances in molecular biology now make it possible for quantitative measurement of the viral load using real-time PCR. Therefore, this study aimed to quantitatively measure the viral load of VZV in the aqueous humor and analyse the correlation between viral load in the aqueous humor and clinical manifestations of VZV anterior uveitis in patients with HZO and ZSH.

MATERIALS AND METHODS

Subjects

The subjects were eight patients (three men and five women; age range 43–71 years (mean 61)) with diagnosed VZV anterior uveitis at Tokyo Medical and Dental University Hospital and Miyata Hospital between December 1999 and September 2007. The clinical diagnosis of VZV anterior uveitis was based on observation of anterior uveitis associated with either HZO or ZSH. After informed consent had been obtained, an aliquot of aqueous humor (0.1–0.2 ml) was obtained from each patient. The research followed the tenets of the Declaration of Helsinki, and the study was approved by the institutional ethics committees of Tokyo Medical and Dental University.

PCR assay

The aqueous humor samples were centrifuged at 3000 rpm for 5 min and used for the following PCR assays: multiplex PCR and real-time PCR.[3] Multiplex PCR was designed to qualitatively measure the genomic DNA of eight human herpes viruses: herpes simplex virus type 1 (HSV-1) and type 2 (HSV-2), VZV, Epstein–Barr virus (EBV), cytomegalovirus (CMV), human herpes virus type 6 (HHV-6), type 7 (HHV-7) and type 8 (HHV-8). DNA was extracted from the aqueous humor samples using a DNA minikit (Qiagen, Valencia, CA, USA). Multiplex PCR was performed using LightCycler (Roche, Basle, Switzerland). The primer sequences and PCR conditions for VZV were as previously described.[4]

Real-time PCR was performed only for HHV, the genomic DNA of which was detected by multiplex PCR. It was performed by using Amplitaq Gold and a Real-Time PCR 7300 system (ABI, Forster City, CA, USA). The primer sequences for VZV (ORF29) used in real-time PCR were designed to use Primer Express (ABI): forward, AACTTTTACATCCAGCCTGGCG; reverse, GAAAACCCAAACCGTTCTCGAG. The probe was FAM-TGTCTTTCACGGAGGCAAAC-ACGT-TAMRA. The following PCR conditions were used: denaturation at 95°C for 10 min, 95°C for 15 s, and 60°C for 60 s for 40 cycles.

Table 1 Clinical findings at initial presentation in patients with varicella zoster virus (VZV) anterior uveitis

Case	Age (years)	Sex	Eye	Initial ocular findings: VA	IOP (mm Hg)	Mutton-fat KPs	Cells in AC	Flare in AC	Pigmentation in the AC angle	Eruption	Time from onset to treatment	Herpes virus DNA: VZV	Others*
1	67	F	Left	0.3	38	+	3+	271	Wide	–	2 months	+	–
2	70	F	Left	0.3	22	+	3+	106	Partial	+	2 weeks	+	–
3	68	F	Right	0.8	10	+	2+	34	None	–	2 months	+	–
4	56	M	Left	1.2	46	+	3+	241	Partial	+	2 months	+	–
5	70	F	Left	1.2	25	–	1+	13	Partial	–	2 months	+	–
6	44	M	Right	0.6	46	–	3+	140	Partial	+	1 week	+	–
7	43	F	Left	1.2	28	–	2+	15	Partial	–	1 month	+	–
8	71	M	Right	0.3	28	–	2+	13	None	+	None	+	–

Aqueous humor samples from eight cases were analysed for human herpes virus DNA by multiplex PCR.
*Herpes viruses excluding VZV, ie, herpes simplex virus type 1 and type 2, Epstein–Barr virus, cytomegalovirus, human herpes virus types 6, 7 and 8.
VA, visual acuity; IOP, intraocular pressure; KPs, keratic precipitates; AC, anterior chamber.

Statistical analysis

Statistical analysis was performed using the Mann–Whitney U test. Statistical significance was set at $p<0.05$.

RESULTS

Clinical manifestations

In four of the patients, there was an episode of skin eruption with neuralgia in the area of the first branch of the trigeminal nerve; this was clinically diagnosed as HZO (table 1). No skin eruptions were observed in the other patients, although they complained of pain near the first branch of the trigeminal nerve, leading to the diagnosis of ZSH. At various intervals after the onset of HZO or ZSH, the patients developed unilateral anterior uveitis. All patients had cells and flare in the anterior chamber, with increased flare values measured by a laser flare meter (Cowa, Tokyo, Japan). Four patients exhibited mutton-fat KPs (table 1), which had brownish pigmentation and were small or medium in size. Three patients with HZO already exhibited iris atrophy and pupil distortion on referral. High intraocular pressure (IOP) was recorded in all patients except in case 3 (table 1). A gonioscopic examination revealed wide, open angles in all patients, and higher pigmentation in the affected eye than the other eye in six of the eight patients. Ophthalmoscopic examinations revealed no significant inflammatory lesions in the retina and choroid. These clinical results led us to a diagnosis of anterior uveitis associated with HZO or ZSH, with paracentesis subsequently performed in order to carry out the PCR analysis.

After confirmation of the presence of VZV in the aqueous humor by multiplex PCR, systemic anti-VZV agents (aciclovir or valaciclovir) and aciclovir ointment were administered for at least 4 weeks together with a topical corticosteroid (eg, betamethasone) and anti-glaucoma agents (eg, timolol and latanoprost). Iris atrophy and pupil distortion developed during the clinical course (fig 1, table 2). The anterior uveitis and high IOP responded well to treatment.

PCR analysis of the aqueous humor

Qualitative PCR (multiplex PCR) detected genomic DNA of VZV but not of other human herpes viruses (HSV-1, HSV-2, EBV, CMV, HHV-6, HHV-7 and HHV-8) in the aqueous humor of all eight patients (table 1). In peripheral blood samples, however, no genomic DNA of any of the eight human herpes viruses, including VZV, was detected in any of the patients.

Quantitative PCR (real-time PCR) detected significant viral loads of VZV DNA in the aqueous humor of the eight patients ranging from 3.8×10^2 to 1.2×10^7 copies/ml (table 2). It is of note that the VZV viral load in the aqueous humor correlated with the intensity of iris atrophy and pupil distortion (table 2, fig 1). Patient 1 had the highest VZV viral load (1.2×10^7 copies/ml) in the aqueous humor and also had the most severe iris atrophy, with multiple wide areas of segmental iris atrophy and a widely dilated pupil (fig 1A, table 2). Patients 2–5 had the second

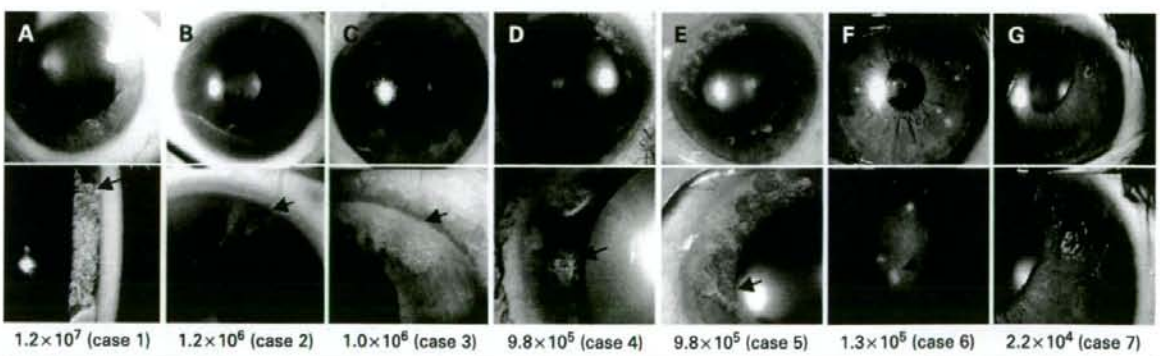

Figure 1 Iris photographs for patients with varicella zoster virus (VZV) anterior uveitis. Slit-lamp photographs are available for seven cases as shown. The numbers indicate the copies of the VZV genomic DNA for each of the aqueous humor samples (copies/ml). Arrows point to areas of iris atrophy. Consent has been obtained for publication of this figure.

Table 2 Virological analysis and ocular findings after treatment of patients with varicella zoster virus (VZV) anterior uveitis

Case	VZV DNA (copies/ml)	Final ocular findings: VA	IOP (mm Hg)	Cells in AC	Flare in AC	Iris atrophy	Extent of iris atrophy (%)	Pupil	Maximum pupil diameter (mm)	Systemic treatment	Follow-up (months)
1	1.2×10^{7}	mm	10	–	13	Wide	40	Distorted, mydriasis	8.1	ACV, ACZ	48
2	1.2×10^{6}	0.9	14	–	8	Segmental	4	Distorted, mild mydriasis	3.4	VCV, ACZ	5
3	1.0×10^{6}	0.8	7	–	5	Segmental	15	Distorted, mydriasis	5.0	VCV	4
4	9.8×10^{5}	0.9	10	–	73	Segmental	20	Distorted, mydriasis	7.9	VCV	12
5	9.8×10^{5}	0.8	20	–	22	Segmental	29	Distorted, mydriasis	7.0	VCV	5
6	1.3×10^{5}	1.5	13	–	6	Circular	1	Normal	2.6	ACV	26
7	2.2×10^{4}	2	16	–	3	Circular	1	Distorted, mild mydriasis	4.3	VCV	13
8	3.8×10^{2}	1.2	12	–	9	None	0	Normal	2.6	ACV, ACZ	4

The copy number of the VZV genome in aqueous humor was evaluated with real-time PCR. The extent of iris atrophy was calculated using Photoshop Elements V2.0.
ACV, aciclovir; ACZ, acetazolamide; mm, motus manus; VCV, valaciclovir.

highest viral loads in the aqueous humor (~1×10^{6} copies/ml), and these patients developed multiple segmental or circular iris atrophy with moderate pupil distortion, although these signs were not as marked as in patient 1 (fig 1B–E, table 2). Patients 6 and 7 had the third highest viral load (10^{5}–10^{4} copies/ml) and exhibited circular iris atrophy with minimum pupil distortion (fig 1F,G). Patient 8 had the lowest viral load. This patient exhibited no iris atrophy and the pupil remained normal throughout the clinical course.

We next examined whether higher viral load in the aqueous humor was significantly associated with the intensity of the iris atrophy and pupil distortion. For this analysis, we separated the patients into two groups: higher viral load (patients 1–5) and lower viral load (patients 6–8). The extent of iris atrophy was significantly ($p<0.05$) larger in the group with higher viral load. In addition, the maximum pupil diameter in the pupil distortion was significantly ($p<0.05$) larger in the group with higher viral load. These results suggest that higher viral load in the aqueous humor is closely associated with the intensity of the iris atrophy and pupil distortion.

DISCUSSION

Human herpes viruses are known to be involved in many ocular pathological conditions, such as keratitis, anterior uveitis and necrotising retinitis. Early treatment with anti-viral agents, based on a rapid and accurate diagnosis of the viral infection in ocular tissues, is clinically important in order to avoid the irreversible tissue damage and visual impairment caused by viral infection. Recent advances in PCR methodology have made it possible to screen for viral infection and further quantify the intensity of the viral infection in ocular inflammatory diseases.[1–3 5–8] Asano *et al*[8] detected herpes virus DNA (VZV or HSV-2) in three cases of acute retinal necrosis using real-time PCR. They monitored viral load in ocular samples of these patients and examined correlations with disease activities of acute retinal necrosis. In this study, we used multiplex PCR to screen for HHV infections (HHV1–8) and real-time PCR to quantify viral load in the aqueous humor of patients with HZO or ZSH.

With multiplex PCR, genomic DNA of VZV was detected in the aqueous humor of all eight patients with HZO and ZSH, and significant VZV viral loads were quantified in the same samples with real-time PCR. After cutaneous lesions or neuralgia, all eight patients with HZO or ZSH developed anterior uveitis, which was characterised by unilateral acute anterior uveitis with high IOP, mutton-fat KPs, trabecular meshwork pigmentation, iris atrophy and pupil distortion, although there were no significant pathological lesions in the cornea or ocular fundus of any of the patients. It is well established that these ocular signs are typical of HZO. The present multiplex PCR data clearly confirm that VZV, but not the other human herpes viruses, is responsible for the anterior uveitis. Furthermore, an important finding in our study was that the extent of iris atrophy and pupil distortion also correlated with the viral load of VZV in the aqueous humor in patients with HZO and ZSH. Unlike iris atrophy, IOP did not correlate with the viral load in the aqueous humor. All but one of the patients had raised IOP ranging from 22 to 46 mm Hg at the onset of anterior uveitis.

This study did not reveal any pathological mechanisms for the correlation of the high VZV viral load with the iris atrophy. However, a previous immunohistological report detected VZV antigens in the stroma and vascular endothelial cells of the iris in anterior uveitis patients with HZO.[9] Another study that used angiography in a patient with HZO showed that there was occlusion of the blood vessels of the atrophic iris.[10] On the basis of previous studies and our present data, we hypothesise that the pathological changes caused by VZV may induce occlusion of the iris vessel leading to iris muscle paralysis, with a net result of iris atrophy and pupil distortion. The higher the viral load in the anterior chamber, the more VZVs there will be in the iris, and thus the more intense the pathological tissue damage.

Early initiation of systemic anti-viral agents, as guided by PCR analysis, would help to avoid, or at least minimise, tissue damage in the iris. Some patients with HZO were only given 1-week systemic anti-viral treatments after the onset of the skin lesions. In these patients, the viral loads of VZV in the aqueous humor were high, and various degrees of iris atrophy and distorted pupil were seen over time. These observations suggest that systemic anti-viral treatments after the onset of HZO are helpful in avoiding or minimising irreversible ocular complications and that qualitative and quantitative PCR can also provide useful information for developing treatments for such patients.

Acknowledgements: We thank Drs Ken Watanabe and Miki Mizukami for technical assistance. This work was supported by a Grant-in-Aid for Young Scientists (B) 18791263 from the Ministry of Education, Culture, Sports, Science and Technology, Japan.

Competing interests: None declared.

Ethics approval: Ethics approval was obtained.

Patient consent: Consent has been obtained for publication of fig 1.

REFERENCES

1. **Yamamoto S,** Tada R, Shimomura Y, *et al*. Detecting varicella-zoster virus DNA in iridocyclitis using polymerase chain reaction. *Arch Ophthalmol* 1995;**113**:1358–9.
2. **Nakamura N,** Tanabe M, Yamada Y, *et al*. Zoster sine herpete with bilateral ocular involvement. *Am J Ophthalmol* 2000;**129**:809–10.

3. **Sugita S,** Shimizu N, Kawaguchi T, *et al*. Identification of human herpesvirus 6 in a patient with severe unilateral panuveitis. *Arch Ophthalmol* 2007**125**:1426–7.
4. **Espy MJ,** Teo R, Ross TK, *et al*. Diagnosis of varicella-zoster virus infections in the clinical laboratory by LightCycler PCR. *J Clin Microbiol* 2000;**38**:3187–9.
5. **De Schryver I,** Rozenberg N, Cassous S, *et al*. Diagnosis and treatment of cytomegalovirus iridocyclitis without retinal necrosis. *Br J Ophthalmol* 2006;**90**:852–5.
6. **Koizumi N,** Yamasaki K, Kawasaki S, *et al*. Cytomegalovirus in aqueous humor from an eye with corneal endotheliitis. *Am J Ophthalmol* 2006;**141**:564–5.
7. **Tran TH,** Rozenberg F, Cassoux N, *et al*. Polymerase chain reaction analysis of aqueous humor samples in necrotising retinitis. *Br J Ophthalmol* 2003;**87**:79–83.
8. **Asano S,** Yoshikawa T, Kimura H, *et al*. Monitoring herpesvirus DNA in three cases of acute retinal necrosis by real-time PCR. *J Clin Virol* 2004;**29**:206–9.
9. **Nakashizuka H,** Yamazaki Y, Tokumaru M, *et al*. Varicella-zoster viral antigen identified in iridocyclitis patient. *Jpn J Ophthalmol* 2002;**46**:70–3.
10. **Marsh RJ,** Easty DL, Jones BR, *et al*. Iritis and iris atrophy in herpes zoster ophthalmicus. *Am J Ophthalmol* 1974;**78**:255–61.

FUNDING AVAILABLE FOR RESEARCH PROJECTS

The Committee on Publication Ethics (COPE) has established a Grant Scheme to fund research in the field of publication ethics. The Scheme is designed to provide financial support to any member of COPE for a defined research project that is in the broad area of the organisation's interests, and specifically in the area of ethical standards and practice in biomedical publishing. The project should have a specific goal and be intended to form the kernel of a future publication.

A maximum sum of £5000 will be allocated to any one project, but applications for smaller sums are welcomed.

The terms and conditions of the Grant are as follows:

- At least one of the applicants must be a member of COPE.
- Calls for applications will be made twice a year with closing dates of 1 December and 1 June. An electronic version of the application form must be sent to the Administrator no later than 12 pm (noon GMT) on the closing date for consideration by COPE Council.
- The application must contain a lay summary of the project, a definition of the question to be posed, sufficient methodological detail to allow assessment of the viability of the project, a clear timeline and a definition of the likely deliverables. A full justification for the sum requested must accompany the application.
- A report on the progress of the research should be presented within one year of the award and at the end of the project. The grant must be used within two years from the date of award, and balance sheets must be forwarded annually. These should be sent to the Administrator. Any remaining funds after two years must be returned.
- It is anticipated that the work stemming from the project will be presented at one of COPE's annual seminar meetings within 2–3 years of the award. Such data may also be published in peer-reviewed journals. Any publications or related presentations at meetings by the recipient emanating in part or whole from COPE's support should be duly acknowledged and copies sent to the Administrator.

Applications are reviewed by a COPE sub-committee. Applicants will be advised of a decision as soon as practicable after the deadline date.

An application form can be obtained by contacting Linda Gough, COPE administrator, at LGough@bmj.com or 020 7383 6602. For more information on COPE, see http://www.publicationethics.org.uk/

The closing date for receipt of applications is 1 December 2007 or 1 June 2008.

Use of multiplex PCR and real-time PCR to detect human herpes virus genome in ocular fluids of patients with uveitis

S Sugita, N Shimizu, K Watanabe, M Mizukami, T Morio, Y Sugamoto and M Mochizuki

Br. J. Ophthalmol. 2008;92;928-932; originally published online 11 Apr 2008; doi:10.1136/bjo.2007.133967